

Article

The Assessment of the Spatiotemporal Characteristics of the Eco-Environmental Quality in the Chishui River Basin from 2000 to 2020

Songlin Zhou ¹, Wei Li ^{1,2,*}, Wei Zhang ¹ and Ziyuan Wang ¹¹ School of Geography and Ecotourism, Southwest Forestry University, Kunming 650224, China² Southwest Research Center for Eco-Civilization, National Forestry and Grassland Administration, Kunming 650224, China

* Correspondence: ww0592@gmail.com; Tel.: +86-135-2930-9372

Abstract: The Chishui River Basin is located in the bordering area of Yunnan, Guizhou and Sichuan provinces, which serves as an important ecological barrier in the upper reaches of the Yangtze River, and plays a leading role in preserving natural environments, protecting water resources, and maintaining soil functions. However, the eco-environmental quality in the basin has encountered serious challenges in recent years, and the conflict between eco-environmental protection and economic development becomes increasingly prominent. Therefore, it is particularly important to quantitatively assess the extent of the eco-environmental changes in this basin. The present study acquired Landsat series remote sensing images based on the Google Earth Engine (GEE) platform, constructed a remote sensing ecological index (RSEI) as the assessment index that reflects the eco-environmental quality using principal component analysis, studied the changing trend in the eco-environmental quality using the Sen–Mann–Kendall trend test, analyzed the spatial clustering distribution patterns of the eco-environmental quality, based on spatial autocorrelation analysis, and applied the geographical detector model to determine the impacts of natural and anthropogenic factors on the eco-environmental quality. We further applied the CA–Markov model to simulate and predict the eco-environmental quality of the basin in 2025. The results showed the following: (1) between 2000 and 2020, the eco-environmental quality of the Chishui River Basin had been greatly improved. The average RSEI value increased from 0.526 in 2000 to 0.668 in 2020, and the percentage of areas belonging to the good or excellent quality category increased from 42.65% to 68.48%. (2) The main drivers of the eco-environmental quality included population density, mean annual temperature, land use type and elevation. The interactive effect between these drivers was significantly higher than that of individual drivers, and thus possessed stronger explanatory power for quality differences. (3) It is predicted that in 2025, the eco-environmental quality of the basin will continue to improve, and the proportion of land areas with good or excellent quality will continuously increase. The present study can provide reference value for local environmental protection and regional planning.

Keywords: remote sensing ecological index; trend analysis; driving force; CA–Markov model; Chishui River Basin



Citation: Zhou, S.; Li, W.; Zhang, W.; Wang, Z. The Assessment of the Spatiotemporal Characteristics of the Eco-Environmental Quality in the Chishui River Basin from 2000 to 2020. *Sustainability* **2023**, *15*, 3695. <https://doi.org/10.3390/su15043695>

Academic Editor: Agnieszka Bieda

Received: 3 January 2023

Revised: 4 February 2023

Accepted: 9 February 2023

Published: 17 February 2023



Copyright: © 2023 by the authors. Licensee MDPI, Basel, Switzerland. This article is an open access article distributed under the terms and conditions of the Creative Commons Attribution (CC BY) license (<https://creativecommons.org/licenses/by/4.0/>).

1. Introduction

The eco-environmental quality refers to the degree of ecological excellence, which can help assess the balance between human activities and the quality of the environment at a specific spatial and temporal scale [1,2]. In recent years, due to the rapid progress of industrialization and urbanization worldwide, arising ecological and environmental problems have greatly halted economic, environmental and social sustainability, causing increasingly prominent conflicts between economic development and environment protection [3]. Therefore, it is important to assess the eco-environmental quality of a specific region, and reveal the driving forces of environmental changes in a scientific manner, in

order to achieve the goal of maintaining ecological balance, addressing land insufficiency issues, and promoting ecological security.

Remote sensing technology (RST) can sample emitted and reflected electromagnetic radiation from the earth's atmospheric, terrestrial and aquatic ecosystems, and provide fast and repetitive coverage of large areas without disturbing the target areas or objects [4–6]. In recent years, with the continuous development of this technology, RST has become more and more widely used in the field of environmental science. However, many studies have assessed the eco-environmental quality based on single indicators. For example, normalized difference vegetation index (NDVI) is often used to assess changes in regional vegetation cover [7,8], land surface temperature (LST) is commonly used to study the urban heat island effect [9], and the modified normalized difference water index (MNDWI) is frequently applied to extract surface water information [10]. However, since changes in the eco-environmental quality are caused by multiple environmental drivers, the use of a single index cannot objectively and comprehensively assess eco-environmental quality. Therefore, models that integrate multiple indicators were gradually developed. For example, EI index system is adapted by the Chinese Ministry of Environmental Protection in the Technical Specifications for Evaluation of Ecological Environment Status (HJ/T 192–2015). The application of the EI index system, however, is limited due to high subjective selection and poor visualization. Given this, Xu and colleagues proposed the Remote Sensing Ecological Index (RSEI), which combines multiple ecological indicators such as greenness, wetness, heat and dryness [11]. RESI has some obvious advantages; for example, it can be conveniently and quickly obtained or measured, and the application of RESI can help assess the eco-environmental quality in an objective, efficient and comprehensive manner. Therefore, it is not surprising that RESI has been widely used in different geographical settings such as cities [12–14], islands [15], mining areas [16,17], and watersheds [18].

There exist some problems, however, for conventional RESI models. For example, a huge amount of data is often generated, accompanied by challenging data preparation, management, and complicated statistical analysis [19,20], and this is especially troublesome for long time-series RESI assessment. Google Earth Engine (GEE), a cloud-based geospatial analysis platform, can effectively perform large-scale and long-time processing of satellite imagery to detect environmental change patterns [21]. Therefore, GEE has been widely applied to analyze land use changes [22,23], identify crop types and boundaries [24,25], evaluate ecosystem services responses to biotic and abiotic disturbances [26,27] and monitor environmental quality and integrity [28].

The Chishui River Basin (27°20′–28°50′ N, 104°45′–106°51′ E) is rich in natural resources and biodiversity, harboring many wild plants and animals categorized as China's rare or endangered species, and functions as an essential component of the ecological barrier in the middle and upper reaches of the Yangtze River [29]. However, in the past decades, large population size, rapid urban development and increasing human pressure has posed serious challenges to the regional environment, and the conflict between economic development and environment protection has been intense. In recent years, the severe ecological and environmental problems in the region have attracted extensive attention from scholars. They have studied the ecological status of the Chishui River basin in terms of hydrological ecology [30,31], ecosystem services [29], landscape pattern [32], and vegetation cover [33], yet studies on the long-term detection of ecological and environmental quality in the Chishui River basin are relatively limited. The present study aims to analyze spatial and temporal changes in regard to the eco-environmental quality of the basin, and is thus important for the future ecological protection and management of the basin. In addition, due to the complexity of the interaction between ecological environment and the human–land relationship in the basin, the relevant role of natural and socio-economic factors on environmental quality is not clear, and it is necessary to investigate the driving forces of the eco-environmental quality in the basin.

Trend analysis is a method commonly used for detecting time-series changes in eco-environmental quality, which includes Theil–Sen slope estimation and Mann–Kendall (MK)

trend analysis. Trend analysis has good robustness, exhibits high resistance to outliers, and represents a prominent way of revealing the long-term trend [34,35]. As the eco-environmental quality is influenced by multiple factors, and many existing studies tend to focus on the impact of individual indicators, but ignore the possible interactions among them, the geographical detector model is applied to detect spatial stratified heterogeneity and reveal the driving factors behind it. Meanwhile, it can help explain the driving factors of the eco-environmental quality, and quantitatively evaluate the individual and combined effects of multiple factors on the eco-environmental quality, which is of great significance to environmental protection and sustainable development [36]. Markov models (Markov) have the advantage of forecasting the long-range and fluctuating data series, and cellular automata (CA) models are often used to simulate spatiotemporal changes. Recently, a combination of CA models and Markov models (CA–Markov) have been used to predict changes in landscape structure [37], vegetation change [38], and land use [39]. Given that eco-environmental quality-related data are raster data with high spatial autocorrelation characteristics, the present study uses a combination of the above-mentioned methods and models by IDRISI in order to predict changes in the eco-environmental quality of the Chishui River Basin.

With the Chishui River Basin as the study object and based on GEE platform, the present study (1) constructed RESI to analyze the spatiotemporal characteristics of the eco-environmental quality in the basin between 2000 and 2020, and a combination of the Theil–Sen estimator and Mann–Kendall trend analysis was applied to analyze the evolution trend in the eco-environmental quality throughout the study period; (2) analyzed the impacts of natural and anthropogenic factors on the eco-environmental quality, and revealed the driving mechanisms based on GeoDetector analysis; and (3) applied CA–Markov models to predict the trend in environmental changes in 2025. The results can help provide scientific basis and theoretical support for eco-environmental protection and sustainable development in the Chishui River Basin.

2. Materials and Methods

2.1. Study Area

The Chishui River, a first-class tributary of the upper reaches of the Yangtze River, originates in Zhenxiong County, Yunnan Province, and is the only tributary of the Yangtze River in China that has not been dammed. The Chishui River serves as an important ecological barrier and water conservation site in the upper reaches of the Yangtze [29]. The Chishui River Basin is located in the bordering areas of Yunnan, Guizhou and Sichuan provinces, spreading over 13 counties and cities of the three provinces (Figure 1). The Chishui River Basin has unique geographical and bountiful resources (e.g., forests, minerals). In addition, this basin is known for rich biodiversity. For example, rare and endangered species, such as *Abies ernestii*, *Alsophila spinulosa* and *Shizothorax grahami*, are found in this basin. The basin contains mountainous and hilly terrain, as well as lakes, streams, reservoirs and wetlands. The basin has typical continental climate (e.g., cold winters and hot summers), and precipitation events mainly occur during summer.

2.2. Data Source

The image data for this study were obtained from the Tier 1 (T1) level datasets of Landsat5(TM) and Landsat8(OLI) provided by the Google Earth Engine (GEE) database. The (T1) level dataset from Google Earth Engine (GEE) database has been geometrically corrected, radiometrically corrected, and atmospherically corrected to meet the geometric and radiometric quality requirements. The spatial resolution is 30 m and the temporal resolution is 16 d.

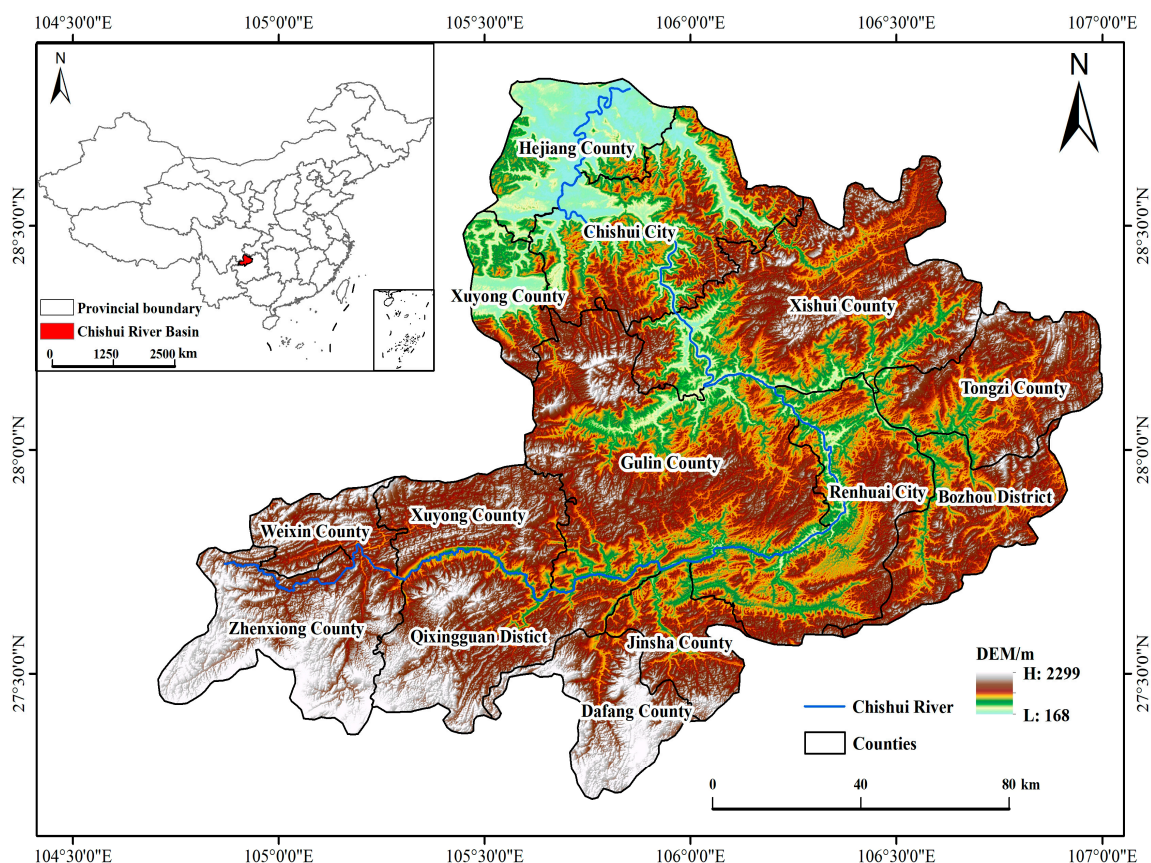


Figure 1. Location of the study area.

Elevation data were obtained from the Aircraft Radar Topography Mission (SRTM) DEM, with a spatial resolution of 30 m; the slope and aspect were extracted from the DEM. Temperature and precipitation data were obtained from the National Earth System Science Data Center (<http://www.geodata.cn/>, accessed on 5 August 2022), with a spatial resolution of 1 km. Soil type (Agrotype) data were obtained from the China Soil Dataset (v1.1) based on the World Soil Database (HWSD) (<https://data.tpdc.ac.cn/>, accessed on 5 August 2022), with a spatial resolution of 1 km. Land use type and GDP data were obtained from the Resource and Environmental Science and Data Center (<https://www.resdc.cn/>, accessed on 5 August 2022). Population density data were obtained from the World Population Density Network (<https://www.worldpop.org/>, accessed on 5 August 2022), with a spatial resolution of 30 m and 1 km. Road and river data were obtained from OpenStreetMap data (<https://www.openstreetmap.org/>, accessed on 5 August 2022).

2.3. Methods

2.3.1. The RSEI Quantification

Based on the GEE platform, the image data of 2000, 2005, 2010, 2015 and 2020 were selected, and the remote sensing images with the imaging time of the target year and 1 year before and after the vegetation growing season (May–October) time range were screened, in order to remove the interference of clouds by cloud masking. To avoid large areas of water that might affect the load distribution of the principal components, the MNDWI water body index was used to mask off the water body information (set at a threshold of 0.2). Finally, median extraction was performed on the image set to eliminate the effect of mask processing and image acquisition time differences to obtain cloud-free median synthetic images of the target year.

The RSEI is quantified by coupling the four ecological indicators, namely, greenness (NDVI), wetness (WET), heat (LST) and dryness (NDBSI) using principal component analysis, where the greenness indicator is represented by the normalized difference vegetation index (NDVI), which represents the growth of vegetation in the study area [40]. The wetness index is represented by the converted moisture component (WET) based on the tasseled cap transformation, which reflects the wetness level of the soil and vegetation [41]; the heat index (i.e., land surface temperature, LST) is an important indicator that reflects ecological processes and climate change [42]; and the dryness index is expressed as the average of two indicators, the bare soil index (SI) [43] and the index-based built-up index (IBI) [44], which reflects the dryness level of the land surface. The formulae and parameters of the four indicators are listed below (Table 1).

Table 1. Formula and reference of the four ecological indicators.

Indicators	Calculation Method	
NDVI	$NDVI = (B_{nir} - B_{red}) / (B_{nir} + B_{red})$	$B_{blue}, B_{green}, B_{red}, B_{nir}, B_{swir1}, B_{swir2}$ represent reflectance in Landsat 5/8 band, respectively; β_i are parameters of Landsat 5/8 bands. SI and IBI represent soil index and building index, respectively; T indicates the bright surface temperature. K1 and K2 are calibration parameters for surface temperature. All parameter values refer to [20].
WET	$\beta_1 B_{blue} + \beta_2 B_{green} + \beta_3 B_{red} + \beta_4 B_{nir} + \beta_5 B_{swir1} + \beta_6 B_{swir2}$	
LST	$LST = T / (1 + (\lambda T / \rho) \ln \epsilon) - 273.13$ $L = gain \times DN + bias$ $T = K_2 / (\ln(K_1 / L + 1))$	
NDBSI	$NDBSI = (SI + IBI) / 2$	
	$SI = [(B_{nir} + B_{red}) - (B_{nir} + B_{blue})] / [(B_{nir} + B_{red}) + (B_{nir} + B_{blue})]$ $IBI = B_{green} / (B_{swir1} + B_{green}) / 2B_{swir2} / (B_{swir1} + B_{nir}) + [B_{nir} / (B_{red} + B_{nir}) + B_{green} / (B_{swir1} + B_{green})]$	

Due to dimensional differences between the four indicators, it is necessary to normalize each indicator, with the calculation method as follows:

$$NI_i = (I - I_{min}) / (I_{max} - I_{min}) \tag{1}$$

NI_i is the normalized index value; I_i denotes the i th image element value of the corresponding index; I_{min} is the minimum value; I_{max} is the maximum value.

Principal component analysis was performed on the normalized four indicators. In order to reduce scale inconsistency, the PC1 results were obtained and served as the remote sensing ecological index $RSEI_0$, which were then normalized to obtain the normalized RSEI.

$$RSEI_0 = PC1[f(NDVI, WET, NDBSI, LST)] \tag{2}$$

$$RSEI = (RSEI_0 - RSEI_{min}) / (RSEI_{0max} - RSEI_{0min}) \tag{3}$$

2.3.2. The RSEI Trend Analysis

The Theil–Sen estimator and Mann–Kendall trend test can be well combined; this combination does not require the data to follow a particular distribution, displays high resistance to data outliers, and thus becomes a prominent method to reveal the long-term trend [45]. The Theil–Sen estimator is computed as follows:

$$\beta = \text{mean}\left(\frac{RSEI_j - RSEI_i}{j - i}\right), 2000 \leq i < j \leq 2020 \tag{4}$$

In this formula $RSEI_i$ and $RSEI_j$ are the RSEI value of year i and year j , respectively. If $\beta > 0$, RSEI reflects an improving trend. If $\beta < 0$, RSEI reflects a declining trend.

The Mann–Kendall trend test is applied to determine the significance of a trend [46]:

$$S = \sum_{i=1}^{n-1} \sum_{j=i+1}^n \text{sign}(RSEI_j - RSEI_i) \tag{5}$$

$$\text{sign}(RSEI_j - RSEI_i) = \begin{cases} +1 & RSEI_j - RSEI_i > 0 \\ 0 & RSEI_j - RSEI_i = 0 \\ -1 & RSEI_j - RSEI_i < 0 \end{cases} \quad (6)$$

$$Z = \begin{cases} (S - 1) / \sqrt{\text{var}(S)}, & S > 0 \\ 0, & S = 0 \\ (S + 1) / \sqrt{\text{var}(S)}, & S < 0 \end{cases} \quad (7)$$

In this formula, var represents variance, and n is the length of the time series. In the present study, the significance level was set as $\alpha = 0.05$. If $|Z| > 1.96$, the trend is prominent. Otherwise, it is not prominent.

2.3.3. The Geographical Detector Model

In order to reveal the driving factors of the eco-environmental quality in the Chishui River Basin, the geographical detector model was included in the present study to help analyze the individual (e.g., through single-factor detection) and combined effects (e.g., through interaction detection) of multiple factors on the eco-environmental quality of the basin [36]. In addition, the selection of these factors was based on relevant studies that focus on the assessment of environmental quality in regard to spatiotemporal dynamics.

Single-factor detection: we calculate the q value of each influencing factor, and explore whether each influencing factor imposes an effect on the eco-environmental quality and the magnitude of the explanatory power. The formula is as follows [36]:

$$q = 1 - \frac{\sum_{h=1}^L N_h \sigma_h^2}{N \sigma^2} \quad (8)$$

In this formula, N_h and N are the number of cells in layer h and the entire region, σ_h^2 and σ^2 are the variance of variable Y in layer h and the whole region, respectively; q is the explanatory power of the indicator factor on RSEI with a range of $[0, 1]$, with larger values indicating a stronger explanatory power on RSEI, and vice versa.

The interaction detection: This method is used to detect the interactive impact between different factors on the eco-environmental quality, and to assess whether their interactive impact enhances or weakens the explanatory power. The five types of interactions are listed below (Table 2).

Table 2. Types of the interactions.

Types of the Interactions	Basis for Judgment
Non-linear weakening	$q(X1 \cap X2) < \min[q(X1), q(X2)]$
Single linear weakening	$\min[q(X1), q(X2)] < q(X1 \cap X2) < \max[q(X1), q(X2)]$
Two-factor enhancement	$\max[q(X1), q(X2)] < q(X1 \cap X2) < q(X1) + q(X2)$
Mutual independence	$q(X1 \cap X2) = q(X1) + q(X2)$
Non-linear enhancement	$q(X1 \cap X2) > q(X1) + q(X2)$

2.3.4. CA–Markov Model

The cellular automaton (CA) is a lattice-dynamic model with discrete spatio-temporal states, which is able to process and operate on complex spatial systems. Its expression is as follows [47]:

$$S_{(t+1)} = f(S_{(t)}, N) \quad (9)$$

In this formula, S is the cellular state; f is the cellular transition rule in local space; t , $t + 1$ are each moment of the cellular; and n is the interval time of 2 moments.

The Markov chain (Markov) model is a spatial distribution model based on the stochastic theory of the system transition probability matrix operation [48]:

$$S_{t+1} = P_{ij} \times S_t \quad (10)$$

In this formula, S_t and S_{t+1} denote the states at t and $t + 1$, respectively; P_{ij} represents the transfer probability matrix.

3. Results

3.1. Analysis of the Overall Characteristics of Eco-Environmental Indicators

The principal component analysis was applied to determine the amount of variance that the four principal components explained (Table 3). Among the loading values of the four components on PC1, those of greenness and wetness are positive, while those of dryness and heat are negative. Therefore, our results match the reality. Meanwhile, since the sign and magnitude of the eigenvalues of the four components in PC2, PC3, and PC4 changed in an unstable manner, they do not have ecological meaning. Therefore, when compared with the other three components, PC1 accounted for over 60% of the total variance in RESI, suggesting that PC1 can effectively integrate the information of the four components and accurately evaluate the eco-environmental quality.

Table 3. Loading values and contribution of each factor to the first principal component.

Year	NDVI	WET	LST	NDBSI	Eigenvalue	Percent Eigenvalue
2000	0.487	0.478	−0.431	−0.591	0.193	62.93%
2005	0.482	0.492	−0.435	−0.580	0.199	63.02%
2010	0.517	0.454	−0.421	−0.591	0.213	64.65%
2015	0.461	0.540	−0.470	−0.575	0.104	69.05%
2020	0.482	0.562	−0.355	−0.571	0.118	70.64%

The four indicators and the mean value of RSEI between 2000 and 2020 can be seen from Figure 2. The results showed that in the past 2 decades, the RSEI of the Chishui River Basin exhibited a continuous upward trend, and the eco-environmental quality of the basin had been greatly improved. For example, the RSEI increased from 0.526 in 2000 to 0.668 in 2020, with an increase rate of 26.97%. Judged based on a single indicator, both the greenness and wetness indicator increased by 0.265 and 0.133, respectively, with an increase rate of 50.96% and 25.53%, respectively; such change trend was consistent with the RSEI trend, indicating that the higher the greenness and wetness is, the better the ecological environment is. Meanwhile, the heat and dryness indicator decreased by 0.073 and 0.128, respectively, throughout the same period; this was opposite to the trend in the RSEI, indicating that the higher the dryness and heat is, the more worrisome the problem of soil desertification and environmental degradation is.

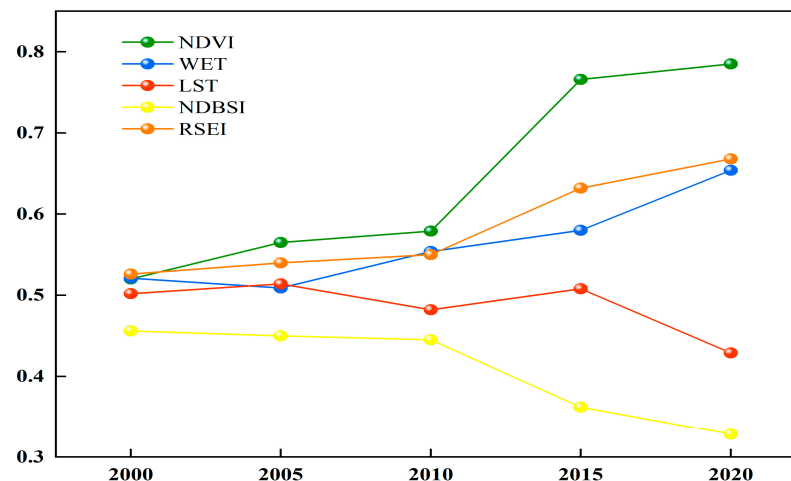


Figure 2. Change in each indicator and RSEI from 2000 to 2020.

3.2. Spatiotemporal Evolution Characteristics of Ecological Environment Quality in the Chishui River Basin

3.2.1. Environmental Quality Grade Structure and Distribution

In order to quantify and visualize the RSEI, the eco-environmental quality in the Chishui River Basin was graded into five levels, namely, bad (0–0.2), poor (0.2–0.4), medium (0.4–0.6), good (0.6–0.8) and excellent (0.8–1), with the corresponding percentage of area determined (Figure 3) and spatial distribution patterns quantified (Figure 4). It can be seen that, (1) between 2000 and 2020, the eco-environmental quality of the Chishui River Basin had been improved significantly. The percentage of areas with good or excellent quality category increased from 42.65% to 68.48%, and the percentage of areas with bad or poor quality decreased from 33.02% to 9.9%; (2) the eco-environmental quality of the Chishui River Basin displayed obvious geographic differentiation patterns, among which the areas with bad and poor eco-environmental quality were mainly distributed in the central and southern areas of the Chishui River Basin, such as Renhuai City, Xishui County, Tongzi County, Zhenxiong County, Qixingguan District and Dafang County. By contrast, the areas with excellent or good quality were mainly distributed in the northwestern regions, such as Gulin County and Chishui City. Over time, the eco-environmental quality of the watershed became significantly improved, and areas with poor or bad quality were mainly concentrated in the central part of the Chishui River Basin, including Renhuai City, Xishui County and Tongzi County.

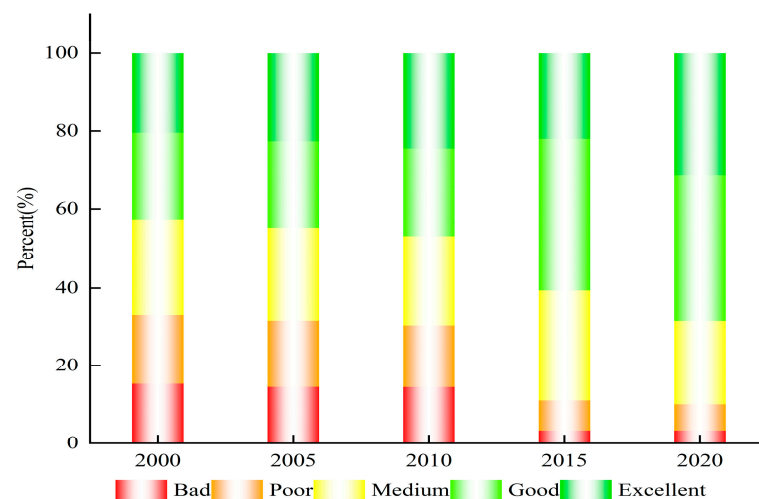


Figure 3. Percentage of area with varying RSEI grade from 2000 to 2020.

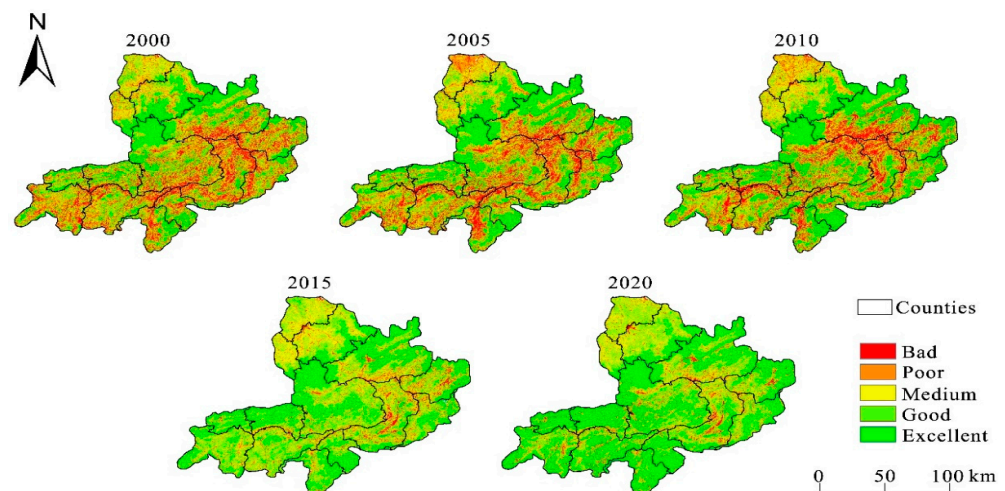


Figure 4. Spatial distribution of RSEI levels from 2000 to 2020.

3.2.2. Analysis of Spatial-Temporal Changes in the Quality Grade

Figure 5 shows the transfer statistics under each category of eco-environmental quality in the Chishui River Basin between 2000 and 2020. In addition to the transfer of each eco-environmental quality category to themselves, the areas in the bad or poor quality category were mostly transferred to each other, and the transfer of areas with bad or poor quality to areas with medium quality increased significantly from 2010 to 2015. Meanwhile, the areas with poor, medium or good quality were transferred to each other, and areas with good or excellent quality were transferred to each other. In total, 2726.98 km² was transferred from areas in the poor category during 2000 and 2020, of which 1045.06 km² was transferred to areas with medium quality, accounting for 38.32% of the total transferred areas. The size of the areas transferred out from areas with medium quality was the largest, with 4692.47 km² transferred out, accounting for 24.33% of the total area being transferred out. Of the total area transferred out, 4692.47 km² was transferred out, accounting for 24.33% of the total area transferred out, of which 2183.58 km² was transferred out to areas with good quality, accounting for 46.53% of the total area transferred out.

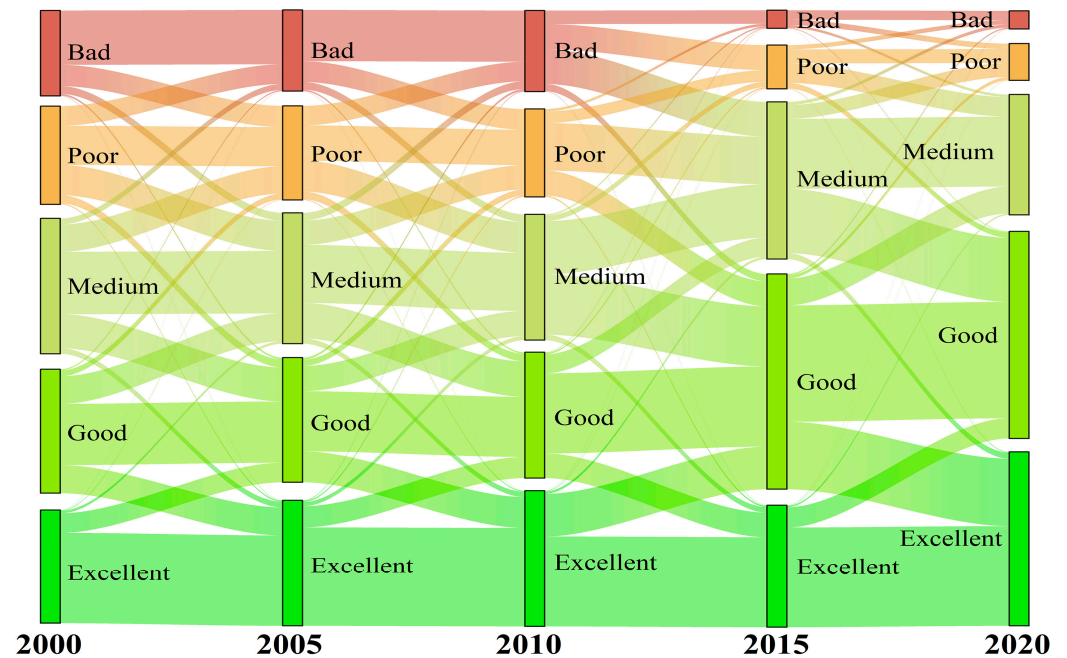


Figure 5. RESI transfer matrix for the Chishui River Basin in 2000–2020.

3.3. Results of Trend Analysis of RSEI and Associated Indicators in the Study Area

A combination of the Theil–Sen estimator and Mann–Kendall trend analysis showed the long-term changing trend in the eco-environmental quality in the Chishui River Basin. Figure 6 displayed the changing trends in RSEI and the four associated indicators, among which the improved area of NDVI and WET accounted for more than 75% and 55% of the improved area, respectively. They were widely distributed in our study area, and had positive impacts on RSEI. By contrast, LST and NDBSI had negative impacts on RSEI, accounting for more than 60% of the total area. The WET and NDVI with positive benefits remarkably increased, while the LST and NDBSI with negative benefits decreased significantly, leading to a net effect of increasing RSEI. Approximately 11.07% of the areas in which RSEI remained stable were mainly distributed in central Renhuai City, northern Dafang County and western Xishui County in the Chishui River Basin. In total, 60.46% of the areas with a slight improvement were widely distributed in all counties, and areas with a significant improvement accounted for only 6.91% of the total area. The degradation area accounted for 28.47%, among which light-degraded area accounted for 27.55%, which was mainly distributed in the whole territory of Chishui City, the north of Gulin County and Xishui County, the north and south of Xuyong County, and the west of Hejiang County.

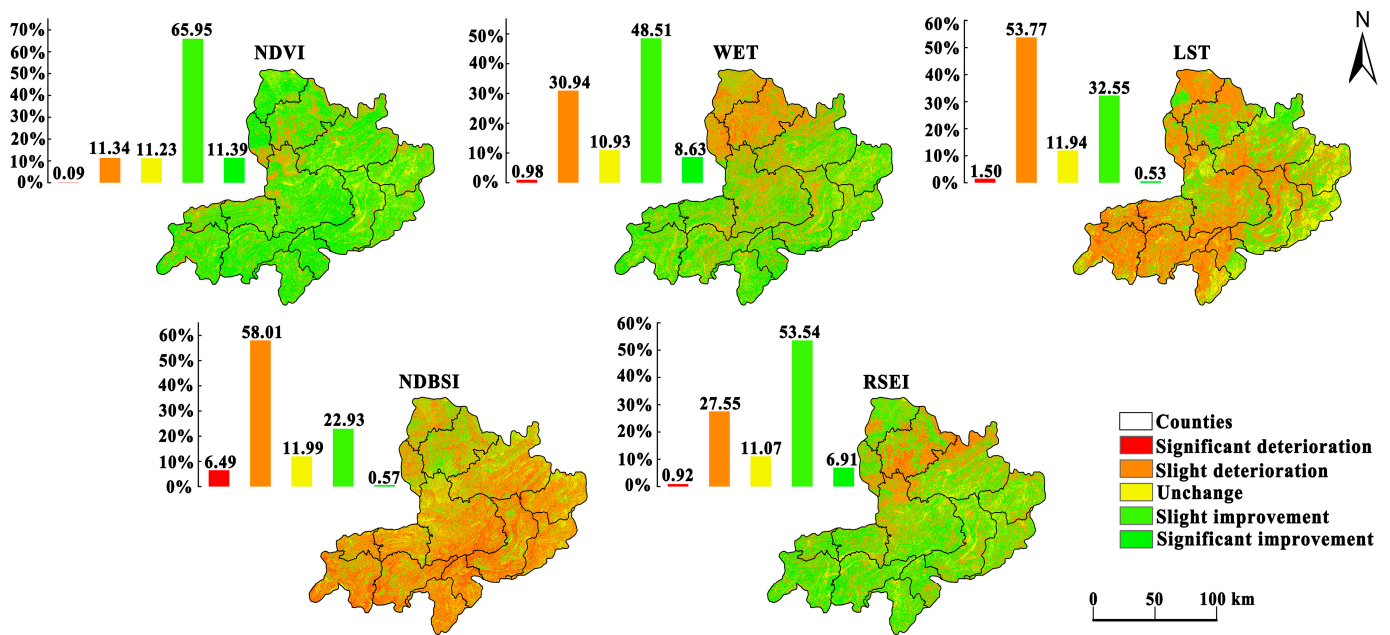


Figure 6. The changing trends of RSEI and the four associated indicators.

3.4. Driving Factors of the Eco-Environmental Quality in the Chishui River Basin

To analyze the driving factors of the eco-environmental quality in the Chishui River Basin, according to available studies [20,29,49], 12 factors that cover natural, socioeconomic and regional accessibility elements were selected as independent variables, and RESI was treated as the dependent variable. The geographical detector model were applied to explore the influence of individual factors and their interactions on the eco-environmental quality in the Chishui River Basin.

3.4.1. The Results of Single-Factor Detection Test

To integrate the spatial resolution and geometric characteristics of different data sources, a $1\text{ km} \times 1\text{ km}$ grid was developed to divide the Chishui River Basin into spatial sample units according to the characteristics of the study area, with the values of RSEI and each independent variable obtained through grid-point sampling and then imported into R. According to the principle of maximizing the q value, the continuous independent variables were then classified based on quantile classification, natural discontinuity point classification and discrete data classification, with the analysis results shown in Figure 7. Clearly, all selected factors had significant effects on RESI spatial differentiation ($p < 0.05$).

The single-factor test showed that eco-environmental quality in the Chishui River Basin was influenced by the combined effect of natural and anthropogenic factors, although the impacts of anthropogenic factors were greater than those of natural factors according to mean q values. The influence of each factor on the spatial distribution of eco-environmental quality was ranked from the highest to the lowest as follows: population density > mean annual temperature > land use type > elevation > GDP > distance from the road > distance from the river > soil type > precipitation > distance from the town > aspect > slope, among which factors such as population density, mean annual temperature, elevation, and land use type were with high importance; meanwhile, factors such as distance from the town, aspect and slope were with low importance. Considering the influence of social factors, such as population growth and economic development, the eco-environmental quality of the Chishui River Basin may be increasingly influenced by anthropogenic activities in the future.

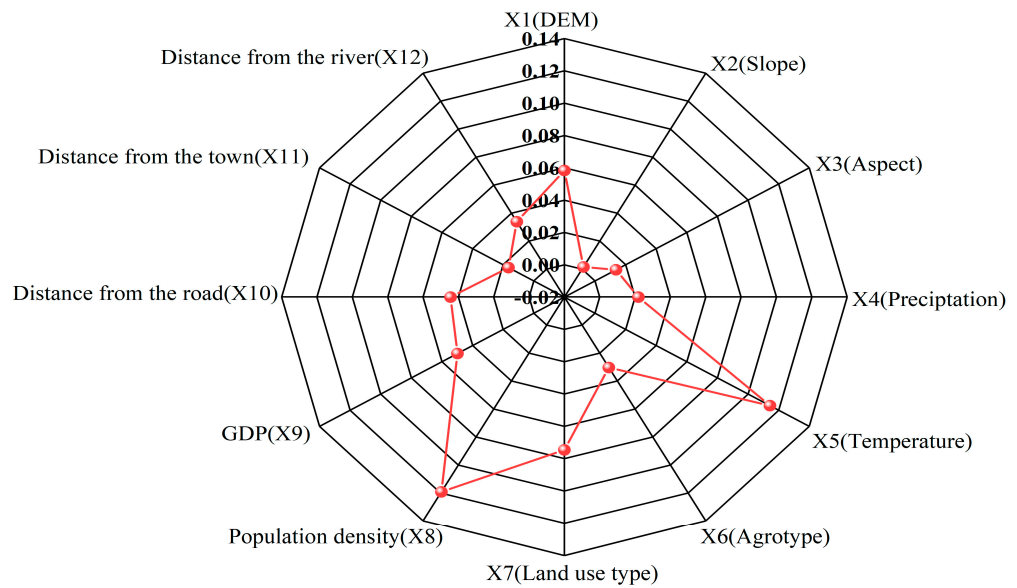


Figure 7. Explanatory power of the influencing factors with respect to the RSEI detection.

3.4.2. The Results of Interaction Detection Test

It can be seen from the interaction detection results that changes in the eco-environmental quality of the Chishui River Basin is the combined result of multiple factors, and the interaction between any two factors has a synergistic enhancing effect compared with the effect of any individual factor on the eco-environmental quality (Figure 8). For example, the interaction between population density and mean annual temperature (0.208), between mean annual temperature and land use type (0.177), and between population density and elevation (0.171) all imposed the largest impacts on the eco-environmental quality. Meanwhile, the impact of the interaction between population density and other factors, or the impact of the interaction between mean annual temperature and other factors, was significantly higher than that of the interaction between other factors. This is consistent with the results of single-factor detection, which indicates that the maximum effect of a single factor is exerted in the interaction of other factors, with the impacts becoming more and more obvious.

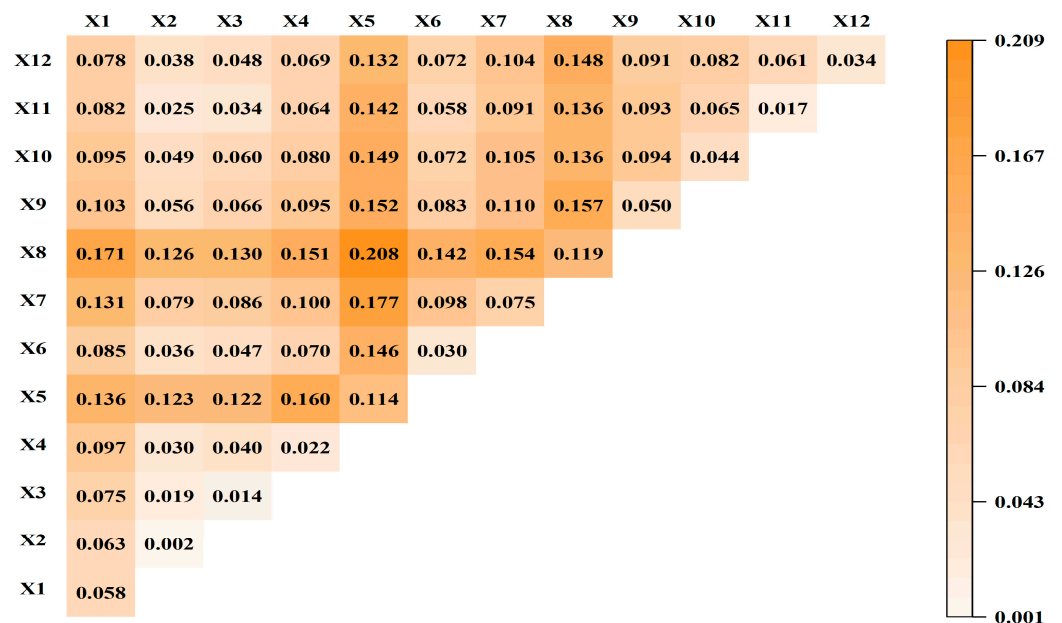


Figure 8. Interaction detection map for each influencing factor.

3.5. CA–Markov Model for Prediction Purpose

Based on the quantified results of RSEI levels in 2010 and 2015, the CA–Markov model was applied to simulate the RSEI levels in 2020 and assess model applicability. The kappa coefficient between the simulated and calculated results was 0.6671 in 2020, suggesting that the model predictions are valid and reliable. The CA–Markov model was further applied to predict the RSEI levels of the Chishui River Basin in 2025 (Figure 9).

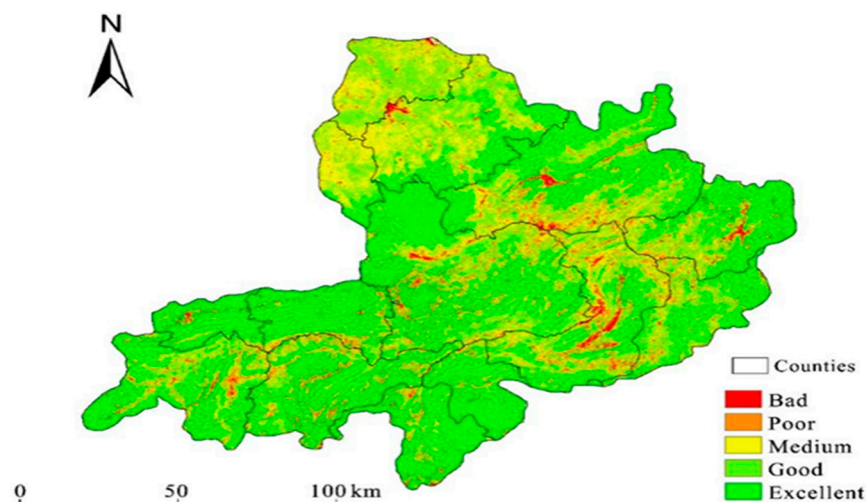


Figure 9. Forecast of ecological quality of the Chishui River Basin in 2025.

Based on the prediction results, the percentage of areas with bad, poor, medium, good and excellent quality in 2025 is 2.92%, 5.87%, 17.96%, 36.71% and 36.54%, respectively. Compared with 2020, the size of the area with bad, poor or medium quality is reduced, whereas the size of the area with good or excellent quality keeps increasing. Therefore, the overall eco-environmental quality in our study areas will be improved in 2025. However, the areas with bad or poor quality are still concentrated in the central and southwest areas of the Chishui River Basin, such as Renhuai City, Xishui County, Gulin County, Zhenxiong County, and Qixingguan District. These areas are known for karst geomorphology characteristics with rocky desertification problems, which are further susceptible to unsustainable mining operations and other anthropogenic perturbations. Therefore, these areas deserve to receive future environmental priorities.

4. Discussion

In the present study, the RSEI index was used to comprehensively assess the eco-environment quality of the basin, which showed obvious geographical differentiation; our findings are consistent with Cai et al. [50], who studied the vegetation cover, and Li et al. [51], who examined the eco-environment grade distribution in this basin. The eco-environmental quality in the Chishui River Basin displays obvious geographical differentiation characteristics. Specifically, the areas with bad or poor quality levels between 2000 and 2010 were mainly distributed in the central and southern areas of the Chishui River Basin, such as Renhuai City, Xishui County, Tongzi County, Zhenxiong County, Qixingguan District, and Dafang County. Zhengxiong County, Qixingguan District, and Dafang County are known for karst geomorphology characteristics with low vegetation cover and rocky desertification problems [49,52]. In addition, these areas had experienced frequent human perturbations. Such natural and human pressures had led to the degradation of the eco-environmental quality (bad or poor quality). As to Renhuai City, Tongzi County and Xishui County, they are located in the middle section of the Chishui River, and thus are susceptible to the influence of topography and slope gradient. This, together with excessive coal, sulfur and iron ore mining activities, led to severe soil erosion [53]. As a result, the eco-environmental quality was also poor in these areas. Since 2012, Sichuan, Yunnan, and

Guizhou provinces have strengthened management measures to control river pollution and improve water quality in the Chishui River Basin, with regional eco-environmental quality greatly improved.

The eco-environmental quality in the Chishui River Basin has improved significantly over recent decades, and the area where the quality has been elevated significantly is much larger than the area where the quality has deteriorated. This is consistent with the findings of Li et al. [54], who studied the trend in ecosystem quality changes in this basin, reflecting the effectiveness of ecological restoration projects. For example, the Returning Farmland to Forest Program and Sustainable Forestry Plantation Program have effectively reduced or minimized the deterioration of soil erosion in our study area, and the eco-environmental quality of Dafang County, Gulin County, Buzhou District, Tongzi County, and Xishui County has been continuously improved, which is consistent with the findings of other researchers who have studied spatiotemporal changes in vegetation coverage in the Chishui River Basin [55].

The eco-environmental quality of the Chishui River Basin is influenced by multiple factors, and the explanatory power of different driving factors on the spatial divergence of the RSEI vary significantly. The results of the single-factor detection test showed that the eco-environmental quality of the Chishui River Basin is mainly influenced by factors such as population density, mean annual temperature, land use type, and elevation. Among anthropogenic factors, land use type determines the fraction of ground covered by green vegetation. For example, the expansion of cities in the watershed region inevitably led to the occupation of a large amount of forest land, grassland and arable land, resulting in a reduction in vegetation cover and a decline in the eco-environmental quality [56]. Meanwhile, population size within the watershed has kept increasing continuously in the past two decades, which is coupled with the rapid development of food processing and electronics industries [57,58]. Indeed, a large amount of surplus labour in rural areas nearby continued to rush into the watershed to seek employment opportunities; this altered the demographic structure of rural households and communities in the watershed, and the increasing population density further imposed a large impact on the eco-environmental quality of the watershed.

Both elevation and annual mean temperature played an important role in affecting the eco-environmental quality. This is because the Chishui River Basin is located in the transitional zone, which connects the Yunnan–Guizhou Plateau with the Sichuan Basin, and exhibits undulating topographic features and a large elevation range. Due to the influence of geographic conditions, vertical divergence in temperature occurs prominently in our study area, which further affects vegetation structure and function. As to multi-factor interactions, the interactions between land use type and mean annual temperature, the interactions between population density and mean annual temperature, between land use type and population density, or between population density and elevation, all play very important roles in affecting the eco-environmental quality. When the findings of the single-factor detection test and interaction detection test are combined, it can be seen that the changes in the eco-environmental quality in the Chishui River Basin are most influenced by these four interactions. In other words, the interactions between natural factors and anthropogenic factors imposed significant impacts over the eco-environmental quality in our study area. Therefore, both the geographic and ecological characteristics of the watershed, as well as the intensity and frequency of human activities, should be fully taken into account in order to protect against environmental harm, and to take necessary measures for the full realization of human well-being, which depends on the quality of the environment.

It should be pointed out that the present study has some limitations. The eco-environment quality evaluation method based on RSEI mainly focuses on greenness, humidity, heat and dryness, but the ecosystem is a complex and diverse system involving many aspects, such as water, biology, topography and other ecological factors. In the future study, more evaluation index factors should be included according to the characteristics of

a specific region [59] so that a rich, systematic and more comprehensive assessment system can be established. In addition, the RSEI lacks empirical data to verify the inverse results, and further efforts should consider adding fieldwork data or comparing published relevant data sets for validation.

5. Conclusions

Based on the GEE cloud processing platform, the study synthesized the annual cloud-free images of the Chishui River basin through image reconstruction, coupled four ecological indicators (i.e., greenness, wetness, dryness and heat) to construct RSEI using principal component analysis, and quantitatively analyzed the spatiotemporal characteristics and distribution patterns of the eco-environmental quality in the Chishui River Basin between 2000 and 2020. The main conclusions of the present research are as follows:

- (1) Between 2000 and 2020, the eco-environmental quality of the Chishui River Basin showed an overall upward trajectory, and this has been especially impressive since 2010. Thanks to the implementation of the policy of returning farmland to forest and the measures of karst rocky desertification control, the eco-environmental quality of the Chishui River Basin has been greatly improved. It is worth mentioning that the governments of Sichuan, Yunnan, and Guizhou provinces have strengthened management measures to control river pollution and improve water quality in the Chishui River Basin, and such regional cooperation is an effective way of promoting environmental conservation.
- (2) The results of geographical detector models showed that population density, mean annual temperature, land type, and elevation were the main drivers of eco-environmental quality. The interactions of two factors enhanced the overall impacts of individual factors, and the multi-factor detector showed that the impact of the interaction between population density, mean annual temperature and other factors was significantly higher than the interaction among other factors.
- (3) The predictive results of the CA–Markov model indicate that the eco-environmental quality of the Chishui River Basin will be further improved in 2025. Specifically, for areas with poor eco-environmental quality, such as Renhuai City, Xishui County, Gulín County and Zhenxiong County that are located in the central and southwest areas of the Chishui River Basin, the protection of fragile environment and the restoration of ecosystem health is a priority for the present and future.

Author Contributions: Conceptualization, S.Z.; Methodology, S.Z. and W.L.; software, S.Z. and W.Z.; validation, Z.W.; formal analysis, S.Z. and W.L.; writing—original draft preparation, S.Z. and W.L.; writing—review and editing, W.Z. and Z.W.; visualization, W.Z.; supervision, S.Z. and W.L.; funding acquisition, W.L. All authors have read and agreed to the published version of the manuscript.

Funding: This research was funded by the National Natural Science Foundation of China (31760175, 31460158), the Scientific Research Fund of Yunnan Provincial Education Department (2023J0722), the Youth Talents of Yunnan Ten Thousand Talents Plan, and the anonymous reviewers for their constructive comments.

Institutional Review Board Statement: Not applicable.

Informed Consent Statement: Not applicable.

Data Availability Statement: The data are available on request from the corresponding author.

Acknowledgments: We would like to thank the editors and anonymous reviewers for their constructive comments and suggestions, which helped to improve the quality of the paper.

Conflicts of Interest: The authors declare no conflict of interest.

References

- Lin, X.; Lu, C.; Song, K.; Su, Y.; Lei, Y.; Zhong, L.; Gao, Y. Analysis of coupling coordination variance between urbanization quality and eco-environment pressure: A case study of the west taiwan strait urban agglomeration, China. *Sustainability* **2020**, *12*, 2643. [\[CrossRef\]](#)
- Sowińska-Świerkosz, B. Application of surrogate measures of ecological quality assessment: The introduction of the Indicator of Ecological Landscape Quality (IELQ). *Ecol. Indic.* **2017**, *73*, 224–234. [\[CrossRef\]](#)
- Mahmoud, S.H.; Gan, T.Y. Impact of anthropogenic climate change and human activities on environment and ecosystem services in arid regions. *Sci. Total Environ.* **2018**, *633*, 1329–1344. [\[CrossRef\]](#) [\[PubMed\]](#)
- Gao, W.; Zhang, S.; Rao, X.; Lin, X.; Li, R. Landsat TM/OLI-Based Ecological and Environmental Quality Survey of Yellow River Basin, Inner Mongolia Section. *Remote Sens.* **2021**, *13*, 4477. [\[CrossRef\]](#)
- Xia, Q.-Q.; Chen, Y.-N.; Zhang, X.-Q.; Ding, J.-L. Spatiotemporal Changes in Ecological Quality and Its Associated Driving Factors in Central Asia. *Remote Sens.* **2022**, *14*, 3500. [\[CrossRef\]](#)
- Yan, Y.; Zhuang, Q.; Zan, C.; Ren, J.; Yang, L.; Wen, Y.; Zeng, S.; Zhang, Q.; Kong, L. Using the Google Earth Engine to rapidly monitor impacts of geohazards on ecological quality in highly susceptible areas. *Ecol. Indic.* **2021**, *132*, 108258. [\[CrossRef\]](#)
- Eckert, S.; Hüsler, F.; Liniger, H.; Hodel, E. Trend analysis of MODIS NDVI time series for detecting land degradation and regeneration in Mongolia. *J. Arid. Environ.* **2015**, *113*, 16–28. [\[CrossRef\]](#)
- Jiang, L.; Liu, Y.; Wu, S.; Yang, C. Analyzing ecological environment change and associated driving factors in China based on NDVI time series data. *Ecol. Indic.* **2021**, *129*, 107933. [\[CrossRef\]](#)
- Karakuş, C.B. The impact of land use/land cover (LULC) changes on land surface temperature in Sivas City Center and its surroundings and assessment of Urban Heat Island. *Asia-Pac. J. Atmos. Sci.* **2019**, *55*, 669–684. [\[CrossRef\]](#)
- Du, Y.; Zhang, Y.; Ling, F.; Wang, Q.; Li, W.; Li, X. Water bodies' mapping from Sentinel-2 imagery with modified normalized difference water index at 10-m spatial resolution produced by sharpening the SWIR band. *Remote Sens.* **2016**, *8*, 354. [\[CrossRef\]](#)
- Xu, H. A remote sensing urban ecological index and its application. *Acta Ecol. Sin.* **2013**, *33*, 7853–7862.
- Boori, M.S.; Choudhary, K.; Paringer, R.; Kupriyanov, A. Spatiotemporal ecological vulnerability analysis with statistical correlation based on satellite remote sensing in Samara, Russia. *J. Environ. Manag.* **2021**, *285*, 112138. [\[CrossRef\]](#) [\[PubMed\]](#)
- Liu, X.; Zhang, X.; He, Y.; Luan, H. Monitoring and assessment of ecological change in coastal cities based on RSEI. *Int. Arch. Photogramm. Remote Sens. Spat. Inf. Sci.* **2020**, *42*, 461–470. [\[CrossRef\]](#)
- Maity, S.; Das, S.; Pattanayak, J.M.; Bera, B.; Shit, P.K. Assessment of ecological environment quality in Kolkata urban agglomeration, India. *Urban Ecosyst.* **2022**, *25*, 1137–1154. [\[CrossRef\]](#)
- Nie, X.; Hu, Z.; Zhu, Q.; Ruan, M. Research on temporal and spatial resolution and the driving forces of ecological environment quality in coal mining areas considering topographic correction. *Remote Sens.* **2021**, *13*, 2815. [\[CrossRef\]](#)
- Pan, J.; Li, H.; Li, Y. Spatiotemporal change analysis of environmental quality in mining areas based on long-term landsat images. *Geocarto Int.* **2022**, 1–16. [\[CrossRef\]](#)
- Wen, X.; Ming, Y.; Gao, Y.; Hu, X. Dynamic monitoring and analysis of ecological quality of pingtan comprehensive experimental zone, a new type of sea island city, based on RSEI. *Sustainability* **2019**, *12*, 21. [\[CrossRef\]](#)
- Yuan, B.; Fu, L.; Zou, Y.; Zhang, S.; Chen, X.; Li, F.; Deng, Z.; Xie, Y. Spatiotemporal change detection of ecological quality and the associated affecting factors in Dongting Lake Basin, based on RSEI. *J. Clean. Prod.* **2021**, *302*, 126995. [\[CrossRef\]](#)
- Cao, J.; Wu, E.; Wu, S.; Fan, R.; Xu, L.; Ning, K.; Li, Y.; Lu, R.; Xu, X.; Zhang, J. Spatiotemporal Dynamics of Ecological Condition in Qinghai-Tibet Plateau Based on Remotely Sensed Ecological Index. *Remote Sens.* **2022**, *14*, 4234. [\[CrossRef\]](#)
- Zhou, J.; Liu, W. Monitoring and Evaluation of Eco-Environment Quality Based on Remote Sensing-Based Ecological Index (RSEI) in Taihu Lake Basin, China. *Sustainability* **2022**, *14*, 5642. [\[CrossRef\]](#)
- Gorelick, N.; Hancher, M.; Dixon, M.; Ilyushchenko, S.; Thau, D.; Moore, R. Google Earth Engine: Planetary-scale geospatial analysis for everyone. *Remote Sens. Environ.* **2017**, *202*, 18–27. [\[CrossRef\]](#)
- Fashae, O.A.; Adagbasa, E.G.; Olusola, A.O.; Obateru, R.O. Land use/land cover change and land surface temperature of Ibadan and environs, Nigeria. *Environ. Monit. Assess.* **2020**, *192*, 109. [\[CrossRef\]](#) [\[PubMed\]](#)
- Venkatappa, M.; Sasaki, N.; Shrestha, R.P.; Tripathi, N.K.; Ma, H.-O. Determination of vegetation thresholds for assessing land use and land use changes in Cambodia using the Google Earth Engine cloud-computing platform. *Remote Sens.* **2019**, *11*, 1514. [\[CrossRef\]](#)
- Stefanidis, S.; Alexandridis, V.; Mallinis, G. A cloud-based mapping approach for assessing spatiotemporal changes in erosion dynamics due to biotic and abiotic disturbances in a Mediterranean Peri-Urban forest. *Catena* **2022**, *218*, 106564. [\[CrossRef\]](#)
- Gu, C.; Zhang, Y.; Liu, L.; Li, L.; Li, S.; Zhang, B.; Cui, B.; Rai, M.K. Qualifying land use and land cover dynamics and their impacts on ecosystem service in central himalaya transboundary landscape based on google earth engine. *Land* **2021**, *10*, 173. [\[CrossRef\]](#)
- Massey, R.; Sankey, T.T.; Yadav, K.; Congalton, R.G.; Tilton, J.C. Integrating cloud-based workflows in continental-scale cropland extent classification. *Remote Sens. Environ.* **2018**, *219*, 162–179. [\[CrossRef\]](#)
- Soh, N.C.; Shah, R.M.; Giap, S.G.E.; Setiawan, B.I.; Minasny, B. High-Resolution Mapping of Paddy Rice Extent and Growth Stages across Peninsular Malaysia Using a Fusion of Sentinel-1 and 2 Time Series Data in Google Earth Engine. *Remote Sens.* **2022**, *14*, 1875.

28. Chen, A.; Yang, X.; Guo, J.; Zhang, M.; Xing, X.; Yang, D.; Xu, B.; Jiang, L. Dynamic of land use, landscape, and their impact on ecological quality in the northern sand-prevention belt of China. *J. Environ. Manag.* **2022**, *317*, 115351. [[CrossRef](#)]
29. Luo, R.; Yang, S.; Wang, Z.; Zhang, T.; Gao, P. Impact and trade off analysis of land use change on spatial pattern of ecosystem services in Chishui River Basin. *Environ. Sci. Pollut. Res.* **2022**, *29*, 20234–20248. [[CrossRef](#)]
30. Xu, S.; Li, S.-l.; Zhong, J.; Su, J.; Chen, S. Hydrochemical characteristics and chemical weathering processes in Chishui River Basin. *Chin. J. Ecol.* **2018**, *37*, 667.
31. Ge, X.; Wu, Q.; Wang, Z.; Gao, S.; Wang, T. Sulfur isotope and stoichiometry-based source identification of major ions and risk assessment in Chishui River Basin, Southwest China. *Water* **2021**, *13*, 1231. [[CrossRef](#)]
32. Li, Y.; Geng, H. Evolution of Land Use Landscape Patterns in Karst Watersheds of Guizhou Plateau and Its Ecological Security Evaluation. *Land* **2022**, *11*, 2225. [[CrossRef](#)]
33. Huang, X.-C.; Yu, L.; Jiang, T.-M.; Jiang, Q.-J.; Xiong, S.-J.; Yang, L.-F. Spatio-Temporal Variations of Vegetation Index in the Chishui River Basin. *J. Southwest Univ.* **2020**, *42*, 139–145.
34. Fan, D.; Ni, L.; Jiang, X.; Fang, S.; Wu, H.; Zhang, X. Spatiotemporal analysis of vegetation changes along the belt and road initiative region from 1982 to 2015. *IEEE Access* **2020**, *8*, 122579–122588. [[CrossRef](#)]
35. Tran, T.V.; Tran, D.X.; Myint, S.W.; Latorre-Carmona, P.; Ho, D.D.; Tran, P.H.; Dao, H.N. Assessing spatiotemporal drought dynamics and its related environmental issues in the Mekong River Delta. *Remote Sens.* **2019**, *11*, 2742. [[CrossRef](#)]
36. Wang, J.; Xu, C. Geodetector: Principle and prospective. *Acta Geogr. Sin.* **2017**, *72*, 116–134.
37. Amir Siddique, M.; Wang, Y.; Xu, N.; Ullah, N.; Zeng, P. The Spatiotemporal Implications of Urbanization for Urban Heat Islands in Beijing: A Predictive Approach Based on CA–Markov Modeling (2004–2050). *Remote Sens.* **2021**, *13*, 4697. [[CrossRef](#)]
38. Wang, H.; Hu, Y. Simulation of biocapacity and spatial-temporal evolution analysis of Loess Plateau in northern shaanxi based on the CA–Markov model. *Sustainability* **2021**, *13*, 5901. [[CrossRef](#)]
39. Matlhodi, B.; Kenabatho, P.K.; Parida, B.P.; Maphanyane, J.G. Analysis of the future land use land cover changes in the gaborone dam catchment using ca-markov model: Implications on water resources. *Remote Sens.* **2021**, *13*, 2427. [[CrossRef](#)]
40. Chu, H.; Venevsky, S.; Wu, C.; Wang, M. NDVI-based vegetation dynamics and its response to climate changes at Amur-Heilongjiang River Basin from 1982 to 2015. *Sci. Total Environ.* **2019**, *650*, 2051–2062. [[CrossRef](#)]
41. Chen, C.; Chen, H.; Liang, J.; Huang, W.; Xu, W.; Li, B.; Wang, J. Extraction of water body information from remote sensing imagery while considering greenness and wetness based on Tasseled Cap transformation. *Remote Sens.* **2022**, *14*, 3001. [[CrossRef](#)]
42. Yang, J.; Duan, S.-B.; Zhang, X.; Wu, P.; Huang, C.; Leng, P.; Gao, M. Evaluation of seven atmospheric profiles from reanalysis and satellite-derived products: Implication for single-channel land surface temperature retrieval. *Remote Sens.* **2020**, *12*, 791. [[CrossRef](#)]
43. Awad, M.; Aldaood, A.; Alkiki, I. Development of a Compressibility Prediction Model Based on Soil Index Properties and Area Under/Bounded by Consolidation and Rebound Curves. *Geotech. Geol. Eng.* **2022**, *40*, 4787–4807. [[CrossRef](#)]
44. Permatasari, A.D.; Prasetyo, S.Y.J. Identifikasi Wilayah Resiko Kerusakan Lahan Terbangun Sebagai Dampak Tsunami Berdasarkan Analisis Building Indices. *J. Transform.* **2022**, *20*, 13–21. [[CrossRef](#)]
45. Sen, P.K. Estimates of the regression coefficient based on Kendall's tau. *J. Am. Stat. Assoc.* **1968**, *63*, 1379–1389. [[CrossRef](#)]
46. Hamed, K.H.; Rao, A.R. A modified Mann-Kendall trend test for autocorrelated data. *J. Hydrol.* **1998**, *204*, 182–196. [[CrossRef](#)]
47. Zhang, Z.; Hu, B.; Jiang, W.; Qiu, H. Identification and scenario prediction of degree of wetland damage in Guangxi based on the CA-Markov model. *Ecol. Indic.* **2021**, *127*, 107764. [[CrossRef](#)]
48. Mokarram, M.; Pourghasemi, H.R.; Hu, M.; Zhang, H. Determining and forecasting drought susceptibility in southwestern Iran using multi-criteria decision-making (MCDM) coupled with CA-Markov model. *Sci. Total Environ.* **2021**, *781*, 146703. [[CrossRef](#)]
49. Wang, K.; Zhang, C.; Chen, H.; Yue, Y.; Zhang, W.; Zhang, M.; Qi, X.; Fu, Z. Karst landscapes of China: Patterns, ecosystem processes and services. *Landsc. Ecol.* **2019**, *34*, 2743–2763. [[CrossRef](#)]
50. Cai, H.; He, Z.; An, Y.; Deng, H. Correlation intensity of vegetation coverage and topographic factors in Chishui watershed based on RS and GIS. *Earth Environ.* **2014**, *42*, 1672–9250.
51. Li, W. Research on the Ecological Environment Quality Change and Influencing Factors of Chishui River Basin in Guizhou Based on Remote Sensing Ecological Index. Guizhou Normal University: Guiyang, China, 2022.
52. Zhang, Z.; Chen, X.; Huang, Y.; Zhang, Y. Effect of catchment properties on runoff coefficient in a karst area of southwest China. *Hydrol. Process.* **2014**, *28*, 3691–3702. [[CrossRef](#)]
53. Cai, S.; Zhou, S.; Cheng, J.; Wang, Q.; Dai, Y. Heavy metals speciation and distribution of microbial communities in sediments from the abandoned Mo-Ni polymetallic mines, southwest of China. *Environ. Sci. Pollut. Res.* **2022**, *29*, 35350–35364. [[CrossRef](#)]
54. Li, G.; Xiao, N.; Li, J. Analysis the trend of ecosystem quality based on ideal reference and key parameters in the Chishui River Basin, China. *Acta. Ecol. Sin.* **2021**, *41*, 7114–7124.
55. Yang, X.; Meng, F.; Fu, P.; Zhang, Y.; Liu, Y. Spatiotemporal change and driving factors of the Eco-Environment quality in the Yangtze River Basin from 2001 to 2019. *Ecol. Indic.* **2021**, *131*, 108214. [[CrossRef](#)]
56. Zhang, S.; Yang, P.; Xia, J.; Qi, K.; Wang, W.; Cai, W.; Chen, N. Research and analysis of ecological environment quality in the Middle Reaches of the Yangtze River Basin between 2000 and 2019. *Remote Sens.* **2021**, *13*, 4475. [[CrossRef](#)]

57. Xu, S.; Lang, Y.; Zhong, J.; Xiao, M.; Ding, H. Coupled controls of climate, lithology and land use on dissolved trace elements in a karst river system. *J. Hydrol.* **2020**, *591*, 125328. [[CrossRef](#)]
58. Xu, S.; Li, S.-L.; Zhong, J.; Li, C. Spatial scale effects of the variable relationships between landscape pattern and water quality: Example from an agricultural karst river basin, Southwestern China. *Agric. Ecosyst. Environ.* **2020**, *300*, 106999. [[CrossRef](#)]
59. Sun, Y.; Liu, S.; Liu, Y.; Dong, Y.; Li, M.; An, Y.; Shi, F.; Beazley, R. Effects of the interaction among climate, terrain and human activities on biodiversity on the Qinghai-Tibet Plateau. *Sci. Total Environ.* **2021**, *794*, 148497. [[CrossRef](#)]

Disclaimer/Publisher's Note: The statements, opinions and data contained in all publications are solely those of the individual author(s) and contributor(s) and not of MDPI and/or the editor(s). MDPI and/or the editor(s) disclaim responsibility for any injury to people or property resulting from any ideas, methods, instructions or products referred to in the content.